We are IntechOpen, the world's leading publisher of Open Access books Built by scientists, for scientists

6,900
Open access books available

185,000
International authors and editors

200M
Downloads

Our authors are among the

154
Countries delivered to

TOP 1%
most cited scientists

12.2%
Contributors from top 500 universities



WEB OF SCIENCE™

Selection of our books indexed in the Book Citation Index in Web of Science™ Core Collection (BKCI)

Interested in publishing with us?
Contact book.department@intechopen.com

Numbers displayed above are based on latest data collected.
For more information visit www.intechopen.com



Chapter

An Adaptive Load Frequency Control Based on Least Square Method

Adelhard Beni Rehiara, Naoto Yorino, Yutaka Sasaki and Yoshifumi Zoka

Abstract

Modern power system becomes a complex system consisted with various load and power stations. Therefore, it may spread into some areas of power system in neighborhood, and so a load frequency control (LFC) is a necessity device to regulate the frequency of the power system by distributing the load to the generating units and controlling tie-line power interchange between areas. The integration of renewable energy sources (RES) into a power grid has presented important issues about stability and security of power system. In such conditions, the use of conventional LFC may not be sufficient to protect the power system against the power changes. In this chapter, an adaptive LFC controller is proposed using the least square method (LSM). The controller adopts an internal model control (IMC) structure in two scenarios, i.e., static controller gain with adaptive internal model and both the adaptive controller gain and adaptive internal model. A two-area power system is used to test and to validate both performance and the effectiveness of this controller through some case studies.

Keywords: adaptive controller, power system stability, LSM, LFC, IMC, res

1. Introduction

Demand load in a power system is continuously varied by the time and the change of the active and reactive power demand has introduced generator-load mismatching power. When the load increases, it will slow down the rotor speed which result drop of the frequency. On the other hand, when the load is reduced, the load frequency will rise. The change of load frequency will directly affect electrical motor performance, further interfering the protection of the system [1].

Smart grid technology is well developed, and it currently has been widely used in the power system operation due to the need for integrating renewable energy to the existing power grid. Penetration of the renewable energy resources such as solar generations and wind turbines to the power grid has introduced significant issues of stability and security of the power system. However, frequency stability is a major issue in the power system operation due to continuous output change of the renewables. Therefore a load frequency control (LFC) is an essential device to back up the automatic generation control (AGC) to keep the frequency stable during power system operation [2].

IntechOpen

The frequency controllers in a power system consist of AGC and LFC systems as primary control and secondary control. An AGC will respond to small changes of frequency in a generator, and an LFC will have to regulate load frequency in a large area of the power system and large change in load frequency which is typically in between ±5 and 6% of the frequency bias [2–5].

In this chapter, adaptive LFC controllers are introduced, where an adaptive IMC model that is repeatedly updated by the least square method (LSM) in real-time operation is proposed. It is shown that the target model is successfully identified and therefore that the proposed LFC controller scheme effectively keeps the system frequency at a desired set point. The effectiveness of the proposed controller is demonstrated by the simulations using a standard LFC model representing two-area interconnected power system.

2. Power system model

2.1 Mathematical modelling of generator

Eq. (1) is well known as a swing equation that describes the rotor dynamics and hence is known as the swing Equation [6, 7]. The internal EMF angle δ is called the load angle that indicates how much power can be transferred:

$$\frac{2H}{\omega_s}\frac{d^2\delta}{dt^2} = P_m - P_e \tag{1}$$

For small perturbation, the swing equation of a synchronous machine will be formed in Eqs. (2) and (3) for its small deviation in speed. Therefore, Laplace transformation of Eq. (3) is shown in Eqs. (4) [6, 7]:

$$\frac{2H}{\omega}\frac{d^2\Delta\delta}{dt^2} = \Delta P_m - \Delta P_e \tag{2}$$

$$\frac{d\Delta\frac{\omega}{\omega_s}}{dt} = \frac{1}{2H}(\Delta P_m - \Delta P_e) \tag{3}$$

$$\Delta f = \frac{1}{2Hs}(\Delta P_m - \Delta P_e) \tag{4}$$

The mathematical model of the generator as formulated in Eq. (4) can be figured in **Figure 1**.

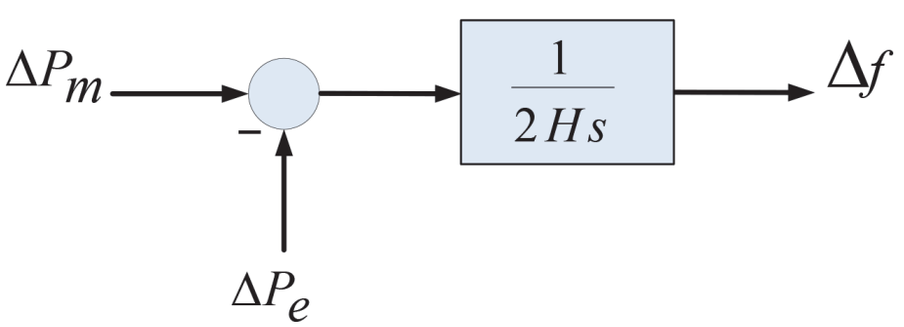


Figure 1.
Block diagram for generator.

2.2 Mathematical modelling of load

The load on a power system consists of a variety of electrical devices which is a resistive or inductive load. The equipment used for lighting purposes and heating are basically resistive in nature, and this kind of load is independent to frequency. On the other hand, rotating devices, such as fans and pumps, are basically a composite of the resistive and inductive components which are dependent to the frequency changes. The speed-load characteristic of the composite load is given by [6, 7]:

$$\Delta P_e = \Delta P_L + D\Delta f \tag{5}$$

where ΔP_L is the load change and $D\Delta f$ is the frequency sensitive load change. D is expressed as percent change in load by percent change in frequency. By adding the load to the generator, block diagram of both load and generator is figured out in **Figure 2**.

2.3 Mathematical modelling for prime mover

The electrical energy is generated inside a power generation by converting the other kind of energy sources by means of a prime mover. The prime mover may be diesel machines, hydraulic turbines at waterfalls, or steam turbines. The model for the turbine relates the changes in mechanical power output ΔP_m to the changes in the steam valve position ΔP_V [6, 7]:

$$G_T = \frac{\Delta P_m}{\Delta P_v} = \frac{1}{1 + T_t s} \tag{6}$$

Figure 3 expresses the prime mover block diagram, where T_t is the turbine constant which has the range in between 0.2 and 2.0 seconds.

2.4 Mathematical modelling for governor

The electrical power will exceed the mechanical power input when the electrical load is suddenly increased. This condition will result in the extraction from the

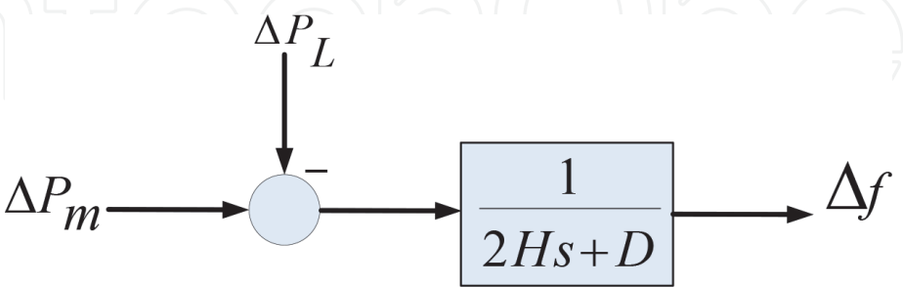


Figure 2.
Generator and load block diagram.

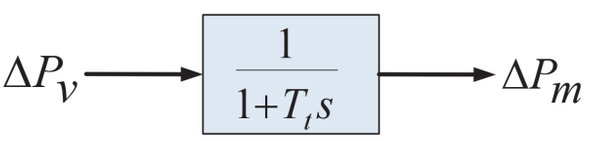


Figure 3.
Block diagram for prime mover.

rotating energy of the turbine. Then the kinetic energy stored in the machine is reduced and slows down the speed of prime mover. Therefore, to compensate the reduced speed, the governor sends a command to supply more volumes of water or steam or gas to increase the prime mover speed.

Speed regulation R is given as the curve slope in **Figure 4**. The typical speed regulation values of generator are in between 5 and 6% from zero to maximum of load [6, 7]:

$$\Delta P_g = \Delta P_{ref} - \frac{1}{R}\Delta f \tag{7}$$

The quantity of ΔP_g is converted to the position of steam valve ΔP_V by a governor time constant T_g. Therefore, the s-domain relation of ΔP_V and ΔP_g is a linear relationship by considering the simple time constant T_g [6, 7] (**Figure 5**):

$$\Delta P_v = \frac{1}{1+T_g s}\,\Delta P_g \frac{1}{1+T_g s} \tag{8}$$

Finally, **Figure 6** summarizes a combining of all of the block diagrams from earlier block diagrams for a single area system.

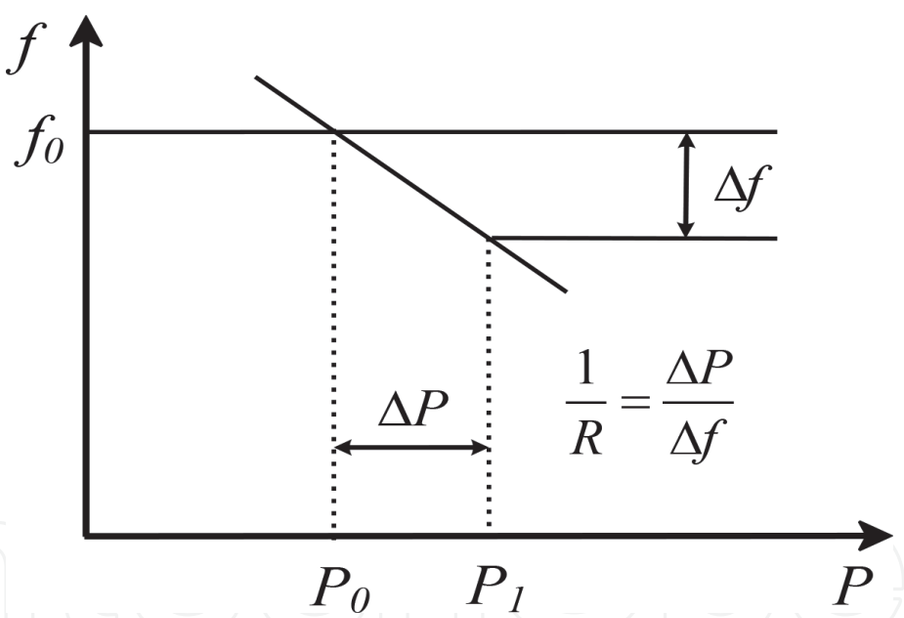


Figure 4.
Speed drop regulation.

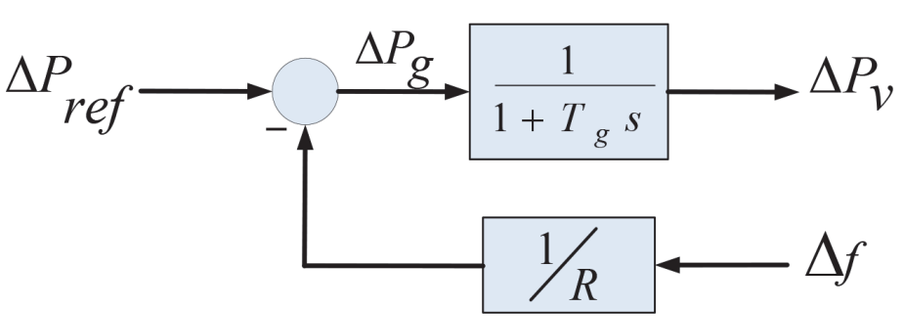


Figure 5.
Block diagram for governor.

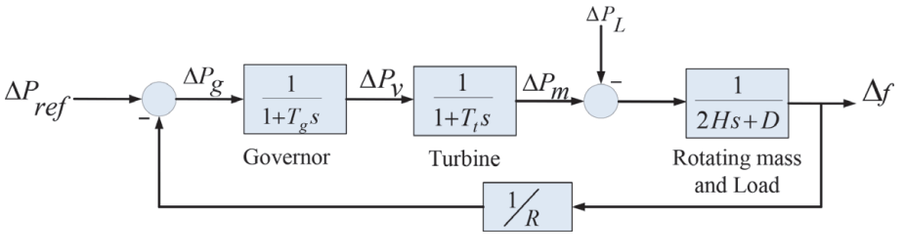


Figure 6.
Completed power system block diagram.

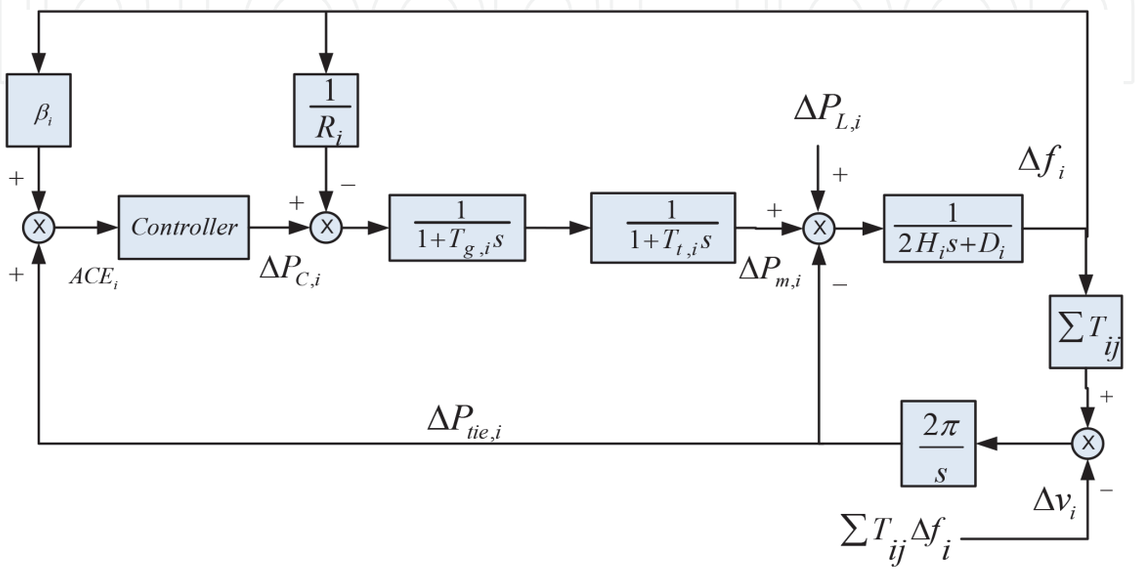


Figure 7.
Power system dynamics.

A completed LFC block diagram for multi-area power system, including controller, frequency bias, and tie-line power change, can be redrawn in **Figure 7** [2–4, 8].

The tie-line power change P_{tie} is calculated for all area n using Eq. (9), and the area control error (ACE) which is a suitable linear combination of frequency f and tie-line power changes for each area is found using Eq. (10) as follows [3, 4, 9]:

$$\Delta P_{tie,i} = \frac{2\pi}{s}\left[\sum_{\substack{j=1 \\ j\neq i}}^{n} T_{ij}\Delta f_i - \sum_{\substack{j=1 \\ j\neq i}}^{n} T_{ij}\Delta f_j\right] \tag{9}$$

$$ACE_i = \Delta P_{tie,i} + \beta_i \Delta f_i \tag{10}$$

A general state-space model is used to describe the power system model as shown in Eqs. (11) and (12):

$$\dot{x}(t) = Ax(t) + Bu(t) + Fw(t) \tag{11}$$

$$y(t) = Cx(t) + Du(t) \tag{12}$$

where $x(t)$, $u(t)$, $w(t)$, and $y(t)$ are the matrices of state variables, input variables, control variable, and output variable, respectively. Four variables of the state variables are $\Delta P_{g,i}$, $\Delta P_{m,i}$, Δf_i, and $\Delta P_{tie,I}$, and the input variables are $\Delta P_{L,i}$ and Δv_i. $\Delta P_{c,I}$ is the control variable, while ACE_i is the output variable.

Due to no direct connection between input and output variables, the feed forward matrix D is removed from the model. Therefore the system matrices of a LFC system are written in Eqs. (13)–(16) [3, 4, 9]:

$$A_i = \begin{bmatrix} -\frac{1}{T_{g,i}} & 0 & -\frac{1}{R_i T_{g,i}} & 0 \\ \frac{1}{T_{t,i}} & -\frac{1}{T_{t,i}} & 0 & 0 \\ 0 & \frac{1}{2H_i} & -\frac{D_i}{2H_i} & -\frac{1}{2H_i} \\ 0 & 0 & 2\pi \sum_{\substack{j=1 \\ j \neq i}}^{N} T_{ij} & 0 \end{bmatrix} \tag{13}$$

$$B_i = \begin{bmatrix} \frac{1}{T_{g,i}} & 0 & 0 & 0 \end{bmatrix}^T \tag{14}$$

$$C_i = \begin{bmatrix} 0 & 0 & \beta_i & 1 \end{bmatrix} \tag{15}$$

$$F_i = \begin{bmatrix} 0 & 0 \\ 0 & 0 \\ -\frac{1}{2H_i} & 0 \\ 0 & -2\pi \end{bmatrix} \tag{16}$$

where $P_{g,i}$, $P_{m,i}$, $P_{L,i}$, $P_{c,i}$, y_i, H_i, d_i, R_i, β_i. T_{ij}, $T_{g,i}$, and $T_{t,i}$ are the output of governor, the prime mover power, the load, the control action, the output of system, the inertia constant, the damping coefficient, the characteristic of speed droop, the bias factor of frequency, the tie-line synchronizing coefficient between reference area i and area j, and the time constant of governor and turbine, respectively.

2.5 System response of power change

Consider a single machine system connected to an infinite bus as shown in **Figure 8**, and its swing equation in steady-state condition can be expressed in Eq. (17) [6]:

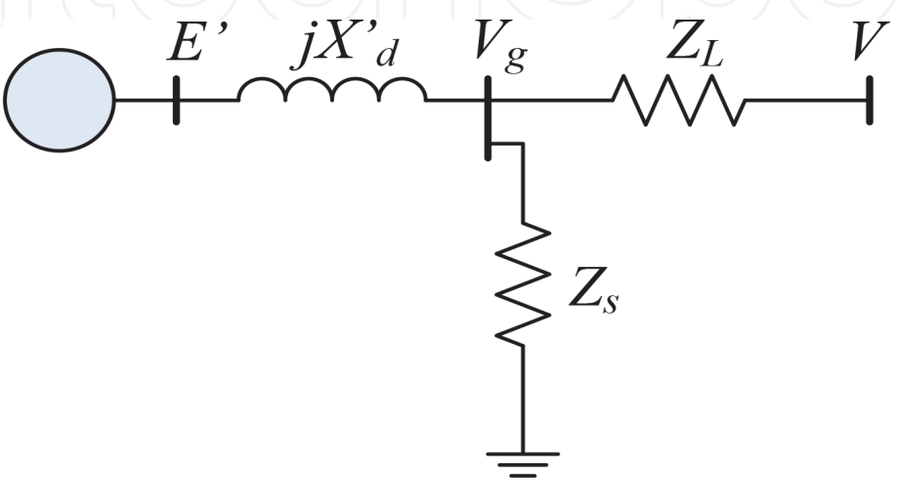


Figure 8.
Single machine system.

$$\frac{H}{\pi f_0}\frac{d^2\delta}{dt^2} = \Delta P_m - \Delta P_{\max}\sin\delta \tag{17}$$

If there is some change in mechanical power input P_m as the result of disturbances or load changes, power angle δ will change to a new state as $\delta = \delta 0 + \Delta\delta$. Then it will further influence swing equation into Eq. (18). The change affects the swing equation in terms of incremental changes in power angle as in Eq. (19):

$$\frac{H}{\pi f_0}\frac{d^2\delta_0}{dt^2} + \frac{H}{\pi f_0}\frac{d^2\Delta\delta}{dt^2} = \Delta P_m - \Delta P_{\max}\sin\delta_0 - \Delta P_{\max}\cos\delta_0\Delta\delta \tag{18}$$

$$\frac{H}{\pi f_0}\frac{d^2\Delta\delta}{dt^2} + \Delta P_{\max}\cos\delta_0\Delta\delta = 0 \tag{19}$$

The quantity of $P_{max}\ cos\ \delta_0$ is known as the synchronizing coefficient P_s which is the slope of power angle curve at δ_0. The root(s) of the second-order differential equation in Eq. (19) can be shown in Eq. (20):

$$s^2 = -\frac{\pi f_0}{H}P_S \tag{20}$$

It can be seen from Eq. (20) that there are possibilities of roots in s-plane when P_s is either positive or negative. A root in the right hand s-plane, where causes system unstable and responses increased exponentially, is gotten when synchronizing coefficient P_s is negative. In other way, two roots will be on j-ω axes of s-plane for P_s negative that causes system responses, oscillatory and undamped with natural frequency as in Eq. (21):

$$\omega_n = \sqrt{\frac{\pi f_0}{H}P_S} \tag{21}$$

3. Controller structure

3.1 Model predictive control

Model predictive control (MPC) is an advance optimal control in the field of control systems engineering. In an MPC, the optimal trajectory movement is given by properly choosing the MPC gain so that the control errors can be minimized.

The objective of the predictive control is to compute the manipulated variable u in order to optimize the output behavior of a controlled plant y. An MPC will use its internal model to calculate the manipulated variable [10] (**Figure 9**).

At a given discrete time k, the plant output is estimated through prediction horizon Np from time $k + 1$ to $k + Np$, and the MPC controller output is predicted by control horizon Nc. The output of the plant is continued to be minimized based on specified objective function which is typically in the form of a quadratic function as shown in Eq. (22) [10]:

$$J(k) = \sum_{m=1}^{Np}\Delta\hat{y}(k+m|k)^{\mathrm{T}}Q\ \ \Delta\hat{y}(k+m|k) + \sum_{m=1}^{Nc}\Delta u(k+m|k)^{\mathrm{T}}R\ \ \Delta u(k+m|k) + \ \ldots$$

$$\ldots + \sum_{m=1}^{Np}u(k+m|k)^{\mathrm{T}}N\ \ u(k+m|k) \tag{22}$$

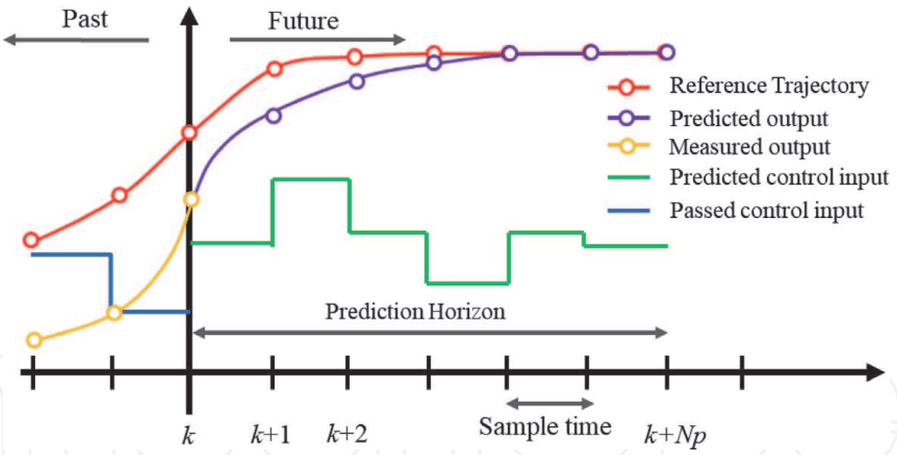


Figure 9.
Principle of MPC.

where N, Q, and R are the error weight matrices of the control action, output system, and rate of change in control action, respectively. $\Delta\hat{y}(k+m|k)$ is the output of plant in prediction, $\Delta u(k+m|k)$ is the change rate in control action under prediction, and $u(k+m|k)$ is the prediction of the action of optimal control, for the measurements given at time $k+m$ from the reference time k.

In order to have optimal result, prediction horizon and control horizon have to be set properly so that the MPC controller can work in high performance. On the other hand, absence of doing this will cause the MPC to lose optimal action that will result in a high overshoot response.

In a short time control horizon, *Nc* will respond with high control action that results in an overshoot after the end of control horizon time. While long time control horizon bring the controller be aggressive and used much energy to accelerate and decelerate the control action in order to keep it constant at set point. In same way, too long prediction horizon *Np* will drop controller performance due to the extra time needed for calculating the trajectory movement, while short time prediction horizon will cause inaccurate calculation of the trajectory.

For a given a linear system in continues time, a system state condition is expressed in Eq. (23) while Eq. (24) shows its formulation for discrete system with sampling time k.

$$\dot{x} = Ax + Bu \tag{23}$$

$$x(k+1) = Ax(k) + Bu(k) \tag{24}$$

$$y(k) = Cx(k) \tag{25}$$

Then the model will be converted to an augmented model so that later the quadratic programming problem with respect to ΔU could be formed easily. Because $u(k) = u(k\text{-}1) + \Delta u(k)$, then Eq. (24) can be rewritten as in Eq. (26), and its state space from is given in Eqs. (27) and (28) [11]:

$$x(k+1) = Ax(k) + Bu(k-1) + B\Delta u(k) \tag{26}$$

$$\begin{bmatrix} x(k+1) \\ u(k) \end{bmatrix} = \begin{bmatrix} A & B \\ 0 & 1 \end{bmatrix} \begin{bmatrix} x(k) \\ u(k-1) \end{bmatrix} + \begin{bmatrix} B \\ 1 \end{bmatrix} \Delta u(k) \tag{27}$$

$$y(k) = \begin{bmatrix} C & 0 \end{bmatrix} \begin{bmatrix} x(k) \\ u(k-1) \end{bmatrix} \tag{28}$$

For the *Np* prediction horizon based on the above equation model, the output of the prediction could be written as:

$$\begin{bmatrix} \hat{y}(k+1) \\ \hat{y}(k+2) \\ \vdots \\ \hat{y}(k+Np) \end{bmatrix} = \begin{bmatrix} CA \\ CA^2 \\ \vdots \\ CA^{Np} \end{bmatrix} x(k) + \begin{bmatrix} CB \\ CAB + CB \\ \vdots \\ \sum_{i=0}^{Np-1} CAB \end{bmatrix} u(k-1) + \ldots \cdots + \begin{bmatrix} CB & 0 & \cdots & 0 \\ CAB + CB & CB & \cdots & 0 \\ \ldots & \ldots & \ldots & \ldots \\ \sum_{i=0}^{Np-1} CAB & \sum_{i=0}^{Np-2} CAB & \cdots & CB \end{bmatrix} \begin{bmatrix} \Delta u(k+1) \\ \Delta u(k+2) \\ \vdots \\ \Delta u(k+Np) \end{bmatrix} \tag{29}$$

Eq. (29) can be simplified as in Eq. (30):

$$\hat{Y} = \Omega X + \Pi u + G\Delta U = F + G\Delta U \tag{30}$$

Then the objective function could be written as:

$$\begin{aligned} J &= \left(\hat{Y} - r\right) + {}^{\mathrm{T}}\left(\hat{Y} - r\right) + \lambda \Delta U^{\mathrm{T}} \Delta U \\ &= (F + G\Delta U - r)^{\mathrm{T}}(F + G\Delta U - r) + \lambda \Delta U^{\mathrm{T}} \Delta U \\ &= \Delta U^{\mathrm{T}}\left(G^{\mathrm{T}} G + \lambda I\right)\Delta U + 2\Delta U^{\mathrm{T}} G^{\mathrm{T}}(F - r) \end{aligned} \tag{31}$$

Therefore, Eq. (31) could be solved efficiently by a quadratic programming.

3.2 Internal model control (IMC)

An IMC controller structure can be seen on **Figure 10** where an internal model is used parallel with the plant. This internal model, which is also called efferent model, used plant model to estimate plant output. It is known that to find the internal model as same as plant model is difficult due to plant dynamics that is not well captured in the modeling part.

In an IMC controller, an efferent model is expected to correct the actual output before it is feedback to the controller. This is the difference between MPC controllers with classical controllers. In order to get maximum performance, the efferent

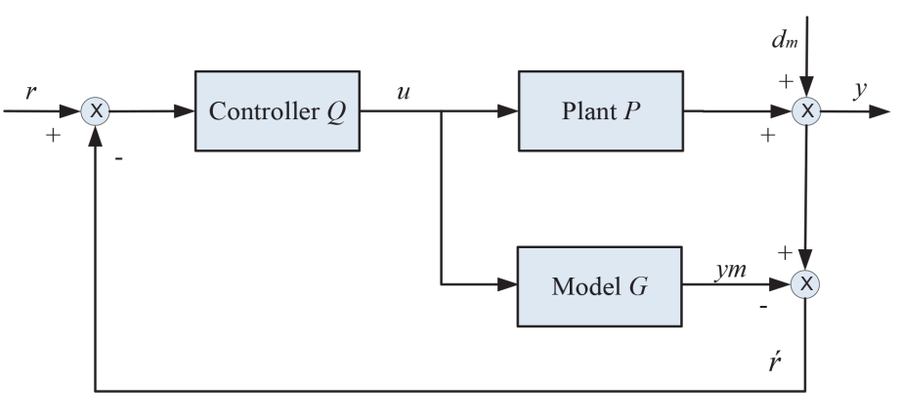


Figure 10.
IMC structure.

model may have input and output relation as close to the real plant model so that the only feedback signal is the disturbance.

As a type of controller, an IMC can control a plant directly. This controller can also be used to tune another controller if it is difficult to be the best parameter for this controller. Based on the IMC structure, this main controller can be any type of controller so that this IMC can be combined with any type of controllers [12]. The control law for an IMC control is written in Eq. (32) to Eq. (34) [13, 14]:

$$y = PQr + (1 - GQ)d \tag{32}$$

$$u = Qr - Qd \tag{33}$$

$$e = (1 - PQ)r - (1 - GQ)d \tag{34}$$

The difference between classical controller and an IMC is that an IMC will correct the actual output before it is fed back. Since an IMC uses the efferent model, the model should be a perfect model to have the highest control performance. The way to provide the model in an IMC can be in forward model, inverse models, combination of both forward and inverse models, or adaptive model.

3.3 Adaptive model structure

Due to highly nonlinearity in a power system, the classical model of power system may not be accurate to configure the real power system. Therefore the other objective of this paper is to find simple model of a load frequency of power system using the least square method (LSM). In order to capture the essential dynamics of power system, a first-order lag model is adopted in this chapter as follows:

$$G(s) = \frac{K}{1 + sT} \tag{35}$$

The power system model, including governor, turbine, and rotating mass and load model as in **Figure 7** will be replaced by the first-order lag model in Eq. (35). Therefore it has become a simple model as formulated in Eq. (36):

$$\Delta f_i = G_i(s) P_{C,i} \tag{36}$$

Expanding Eq. (35) gives

$$\Delta \dot{x}_i = A_i x_i + B_i u_i \tag{37}$$

$$\Delta \dot{f}_i = -\frac{1}{T_i}\Delta f_i + \frac{K_i}{T_i}\Delta P_{C,i} = A_i \Delta f_i + B_i \Delta P_{C,i} \tag{38}$$

For discrete time system, the above equation can be described in a matrix form as follows:

$$\begin{bmatrix} \Delta f_i(k+1) \\ \Delta f_i(k+2) \\ \vdots \\ \Delta f_i(k+M) \end{bmatrix} = [A_i] \begin{bmatrix} \Delta f_i(k) \\ \Delta f_i(k+1) \\ \vdots \\ \Delta f_i(k+M-1) \end{bmatrix} + [B_i] \begin{bmatrix} \Delta P_{C,i}(k) \\ \Delta P_{C,i}(k+1) \\ \vdots \\ \Delta P_{C,i}(k+M-1) \end{bmatrix} \tag{39}$$

Consider a linear equation of least square method $y = Hx$; a solution for minimizing the error can be written as [15, 16]:

$$J(x) = \|y - Hx\|^2 \tag{40}$$

Then expanding $J(x)$ gives

$$\begin{aligned} J(x) &= (y - Hx)^{\mathrm{T}}(y - Hx) \\ &= y^{\mathrm{T}}y - y^{\mathrm{T}}Hx - x^{\mathrm{T}}H^{\mathrm{T}}y + x^{\mathrm{T}}H^{\mathrm{T}}Hx \\ &= y^{\mathrm{T}}y - 2y^{\mathrm{T}}Hx + x^{\mathrm{T}}H^{\mathrm{T}}Hx \end{aligned} \tag{41}$$

Taking the derivative for the $J(x)$ gives

$$\frac{\partial}{\partial x}J(x) = -2H^{\mathrm{T}}y + 2H^{\mathrm{T}}Hx \tag{42}$$

Minimizing the derivative by setting it to zero gives

$$H^{\mathrm{T}}Hx = H^{\mathrm{T}}y \tag{43}$$

If $H^{\mathrm{T}}H$ is invertible, then the least square solution is given in Eqs. (44) and (45) for its simple form:

$$x = \left(H^{\mathrm{T}}H\right)^{-1}H^{\mathrm{T}}y \tag{44}$$

$$x = H^{\dagger}y \tag{45}$$

The least square solution for the discrete time system of the power system model is shown in Eq. (46).

$$\begin{bmatrix} \Delta f_{i,k+1} \\ \\ \vdots \\ \Delta f_{i,k+M} \end{bmatrix} = \begin{bmatrix} \Delta f_{1,k} & \cdots & \Delta f_{n,k} & \Delta P_{C1,k} & \cdots & \Delta P_{Cm,k} \\ \vdots & & \vdots & \vdots & & \vdots \\ \vdots & & \vdots & \vdots & & \vdots \\ \Delta f_{1,k+M-1} & \cdots & \Delta f_{n,k+M-1} & \Delta P_{C1,k+M-1} & \cdots & \Delta P_{Cm,k+M-1} \end{bmatrix} + \begin{bmatrix} A_{i,1} \\ \vdots \\ A_{i,n} \\ B_{i,1} \\ \vdots \\ B_{i,m} \end{bmatrix} \tag{46}$$

where $H^{\dagger}$ is the pseudo inverse of the H matrix. A and B matrices are taken from the LFC state-space model, and ACE is selected as input u to the LFC controller.

3.4 Model simplification

In order to adopt the least square solution into the internal model of the LFC system, the complex system of the LFC is likely to be reduced into a first-order model. After the disturbance is entering the LFC system, generations are expected to change as fast as possible to meet the load demand. This expectation may not be achieved due to slow response of governor and turbine operations. For these

purposes, both turbine and generator responses are neglected to derive a simple expression for the time response.

Considering an LFC model in **Figure 11**, the model in steady-state condition at $\Delta P_L = 0$ will be a third-order transfer function as written in Eq. (47):

$$\Delta f = \left[\frac{K_g K_t K_p}{\left(\frac{K_g K_t K_p}{R} + (sT_g + 1)(sT_t + 1)(sT_p + 1)\right)}\right]\frac{-\Delta P_L}{s} \tag{47}$$

where K_g, K_t, and K_p are a constant of the governor, turbine, and power system, respectively.

Typically in a LFC system, power system time constant is relatively higher than governor and turbine time constant as described in Eq. (48). Therefore both governor and turbine time constant are negligible, and by adjusting $K_g K_t = 1$, Eq. (47) is simplified to be a first-order system in Eq. (49):

$$T_g < T_t << T_p \tag{48}$$

$$\Delta f = \left[\frac{K_p}{\left(\frac{K_p}{R} + (sT_p + 1)\right)}\right]\frac{-\Delta P_L}{s} \tag{49}$$

The first-order system effectively reduced the unexpected response. An example of system responses of first-order and third-order systems is given in **Figure 12**.

The dynamics response of a frequency control means how the frequency is immediately corrected after the disturbance and before the system reaches new steady-state condition [17]. In this case, a static first-order model may not solve the LFC problem since the disturbance is fluctuated by the time. Therefore an adaptive model of first-order system is suggested to be used in solving this problem.

3.5 Computational procedure

Power system model is expressed in a first-order lag system. The way to build the model can be a combination of either inertia constant and damping or a gain and time constant. In this case, the second combination will be used to provide the power system model using the least square method. The power system equation can be written as follows.

Block diagram of the adaptive LFC system is shown in **Figure 13** as rewritten from [1]. The adaptive internal model is utilized to provide an update model of the power system, and the model is generated by using a LSM method. The proposed adaptive LFC controller uses MPC controller as its main controller combining with an adaptive efferent model as the internal model.

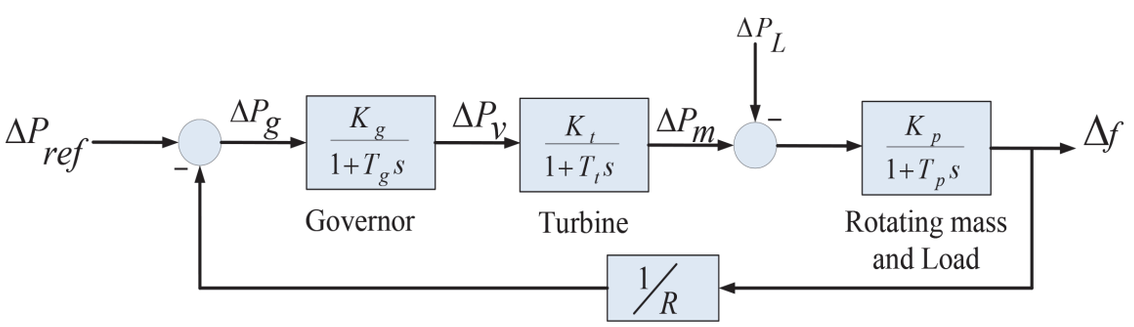


Figure 11.
Power system model.

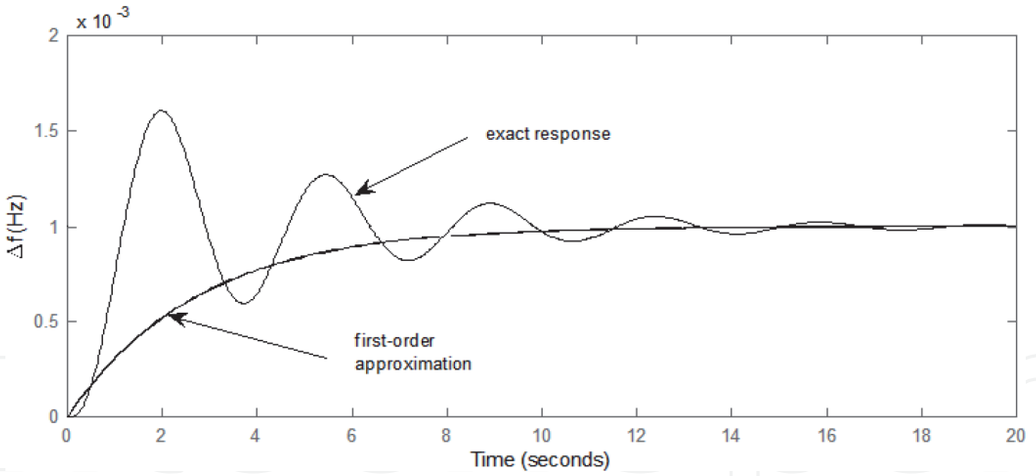


Figure 12.
First- and third-order system responses.

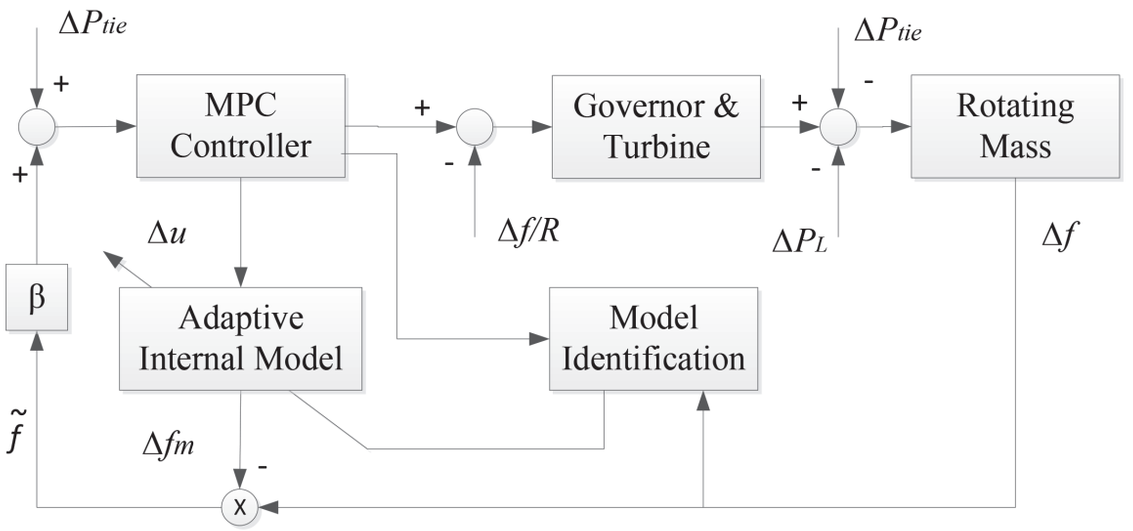


Figure 13.
Adaptive LFC system using IMC structure.

Algorithm 1: **IMC with adaptive model (type 1)**	**Algorithm 2:** **IMC with adaptive model and controller (type 2)**
1. set disturbances and noises	1. set disturbances and noises
2. configure presetting model	2. configure presetting model
3. ⋮	3. ⋮
4. for j = 1 to simulation time	4. for j = 1 to simulation time
5. ⋮	5. ⋮
6. for i = 1 to n-area	6. for i = 1 to n-area
7. calculate Δu	7. calculate Δu
8. upgrade state matrix Δ	8. upgrade state matrix Δ
9. if j = desired time then	9. if j = desired time then
10. update K & T by LSM	10. update K & T by LSM
11. change internal model	11. change internal model
12. end	12. define new MPC gain K_{mpc}
13. calculate model output Δym	13. end
14. correct signal $\Delta = \Delta y - \Delta ym$	14. calculate model output Δym
15. ⋮	15. correct signal $\Delta = \Delta y - \Delta ym$
16. end	16. ⋮
17. end.	17. end
	18. end.

In order to reach the best controller solution, the simulation will be done using the given algorithms. IMC type 1 includes the adaptive internal model, while in IMC type 2, controller gain K_{mpc} is also updated with the change of internal model. Therefore, IMC type 2 uses an algorithm of both adaptive internal model and adaptive MPC controller.

4. Controller test

The investigated power system consists of a two-area power system which is modified from a three-area poser system in [2–4, 9, 18]. The controller performance is tested by comparing a classical MPC controller and the proposed adaptive IMC controller. System configuration is based on **Figure 7** where the system parameter is shown in **Table 1**.

The proposed adaptive LFC controller type 1 and type 2 will be computed as follows. The gain K from P_C to Δf in the detailed model is set to 66.5, which is presetting the value for each area. An initial value of the time constant T is chosen as the same value as the power system model of **Figure 14**, which is set equal to 1. Those will be updated online based on system identification method starting from t = 20.

The main controller for the proposed controller is an MPC controller which at initial condition is set as the same as the existing controller. Prediction horizon Np = 10 and control horizon Nc = 2 are applied to both existing and proposed controllers. In the whole of simulation period, the existing MPC controller gain is not change where computed off line in the beginning before simulation is started.

Area	D [pu/Hz]	$2H$ [pu s]	R [Hz/pu]	T_g [s]	T_t [s]	β [pu/Hz]	T_{ij} [pu/Hz]
1	0.016	0.2017	2.73	0.06	0.44	0.3827	T_{12} = 0.20
2	0.015	0.1247	2.82	0.07	0.30	0.3692	T_{21} = 0.20

Table 1.
System parameters.

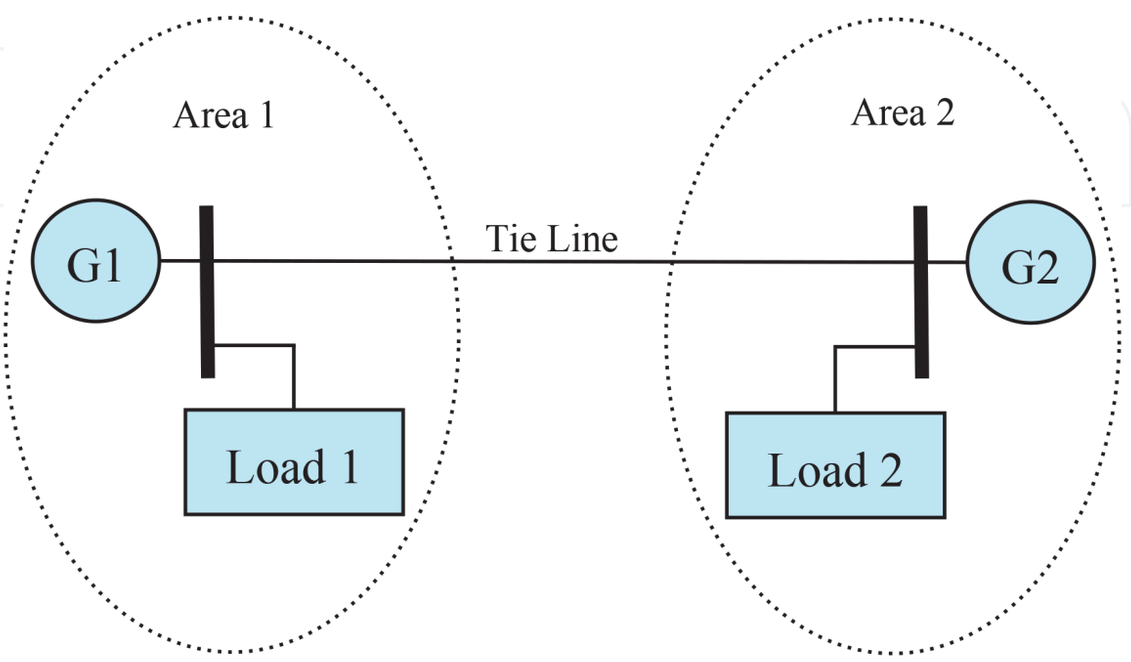


Figure 14.
Multi-area power system configuration.

Case	Disturbance	
	Random	Step change
1	Applied	Not applied
2	Applied	0.2 pu.
3	Applied	−0.1 pu.

Table 2.
Disturbance setting.

Three different cases are performed in simulations under disturbance setting as in **Table 2**. The disturbances are load changes which are imposed by white noises. The random disturbance is white noises with a maximum magnitude about 0.05 pu, while the step disturbance is a sudden change of load. The step disturbance is assumed as the action of economic load dispatching which is applied at t = 40 for case II and case III in addition to the white noise.

4.1 Simulations

A. Case 1.

Simulation results are shown in **Figure 15** for Δf responses and in **Figure 16** for ΔPm responses. In this case, only random disturbance is applied. It is observed that the adaptive controllers both type 1 and type 2 show slightly better performances compared to the existing MPC:

B. Case 2.

The step disturbance about 0.2 pu is applied at t = 40 s in addition to the random disturbance. The results are shown in **Figure 17** for Δf responses and in **Figure 18** for ΔPm responses.

A better performance is observed. It is noted that although the adaptive controllers are a much simpler configuration compared with the existing controller, the control performance is even better. This is an advantageous feature of the proposed method.

C. Case 3.

In this case, step disturbance about −0.1 pu. which is applied at t = 40 s assumed that load is released at t = 40 s including the random disturbance. The results are shown in **Figure 19** for Δf responses and in **Figure 20** for ΔPm responses.

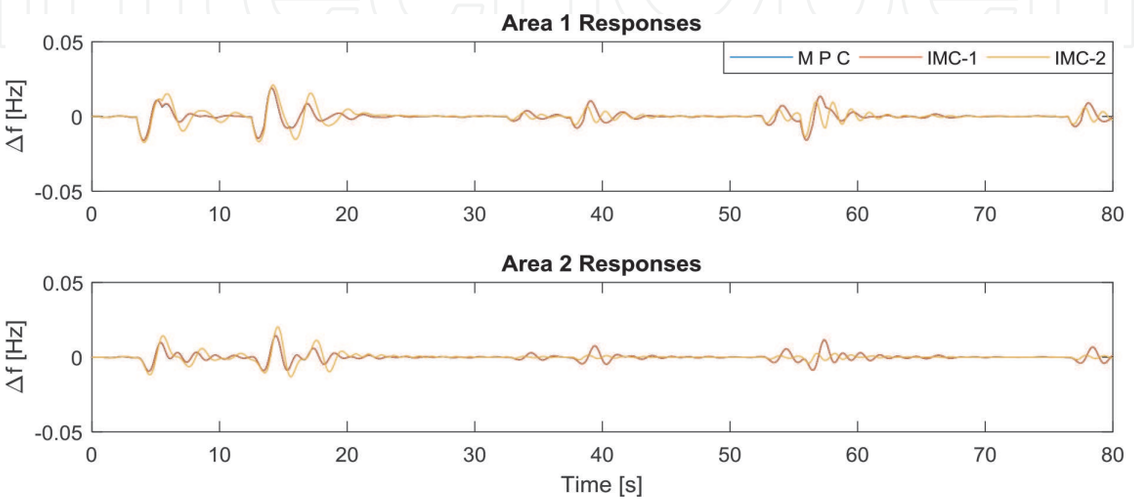


Figure 15.
Case 1: Δf responses.

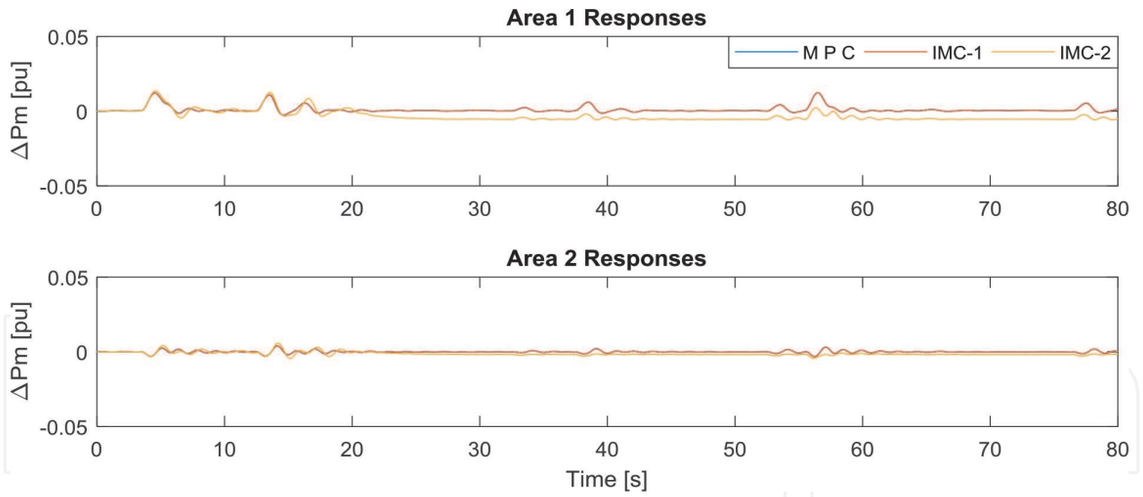


Figure 16.
Case 1: ΔP_m responses.

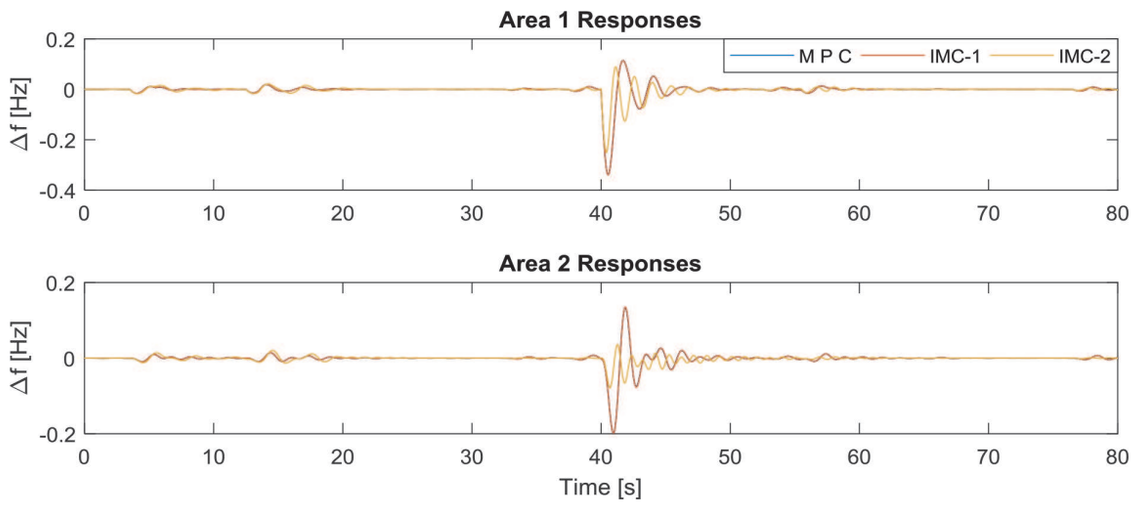


Figure 17.
Case 2: Δf responses.

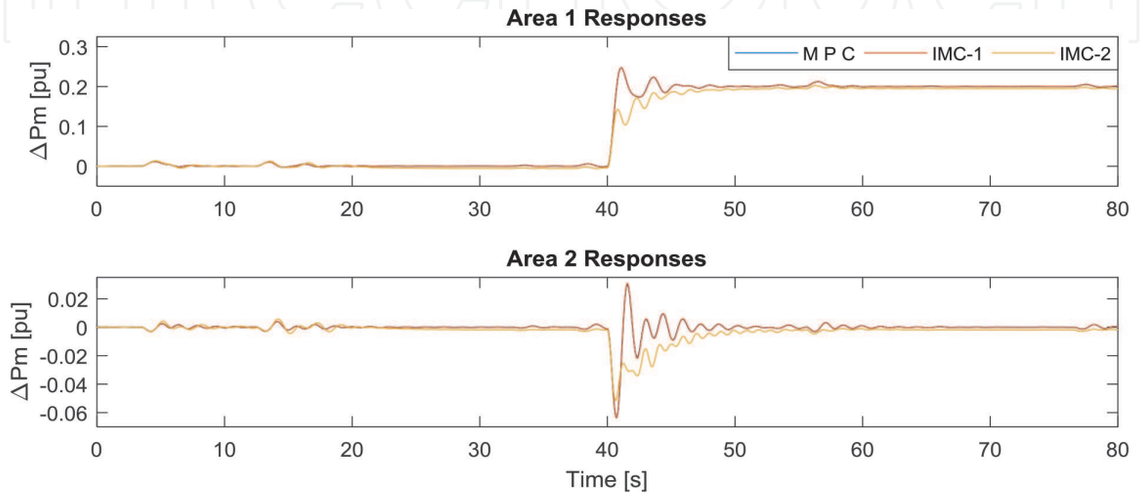


Figure 18.
Case 2: ΔP_m responses.

The similar performance is shown. It is noted that the adaptive controllers can handle incoming disturbance and also released disturbance with even better performance compared to the existing controller.

4.2 Evaluations

Figures 21–24 show how the internal model parameters are identified. It is observed from **Figures 21** and **23** that initial gain K is updated as soon as the model identification process is completed at t = 20, which are consistent values based on the LSM. In the same way, **Figures 22** and **24** show that the initial time constants T are updated very slightly around 1.0. Those values are continuously updated around the converged values.

LFC system based of IMC-1 is equivalent to the existing MPC controller in some cases, while the performance of IMC type 2 is even better in all areas and all cases. **Tables 3** and **4** list measured values of the overshoot for the step disturbance and the standard deviations of both frequency and prime mover responses for all cases. It is seen from the tables that the performance of the proposed adaptive LFC controllers is equivalent or better than the conventional MPC controller. This implies that the adaptive LFC controllers can successfully identify the target model

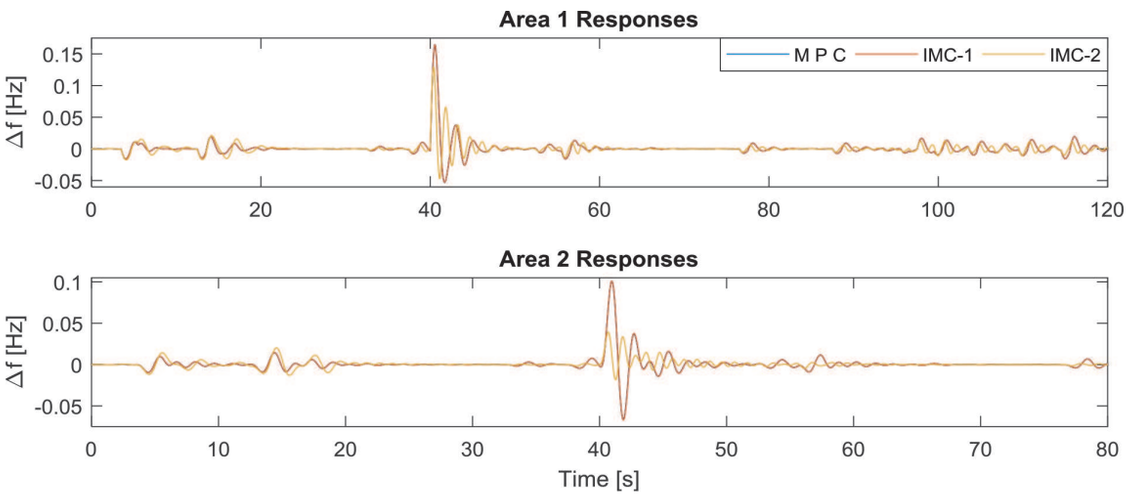


Figure 19.
Case 3: Δf responses.

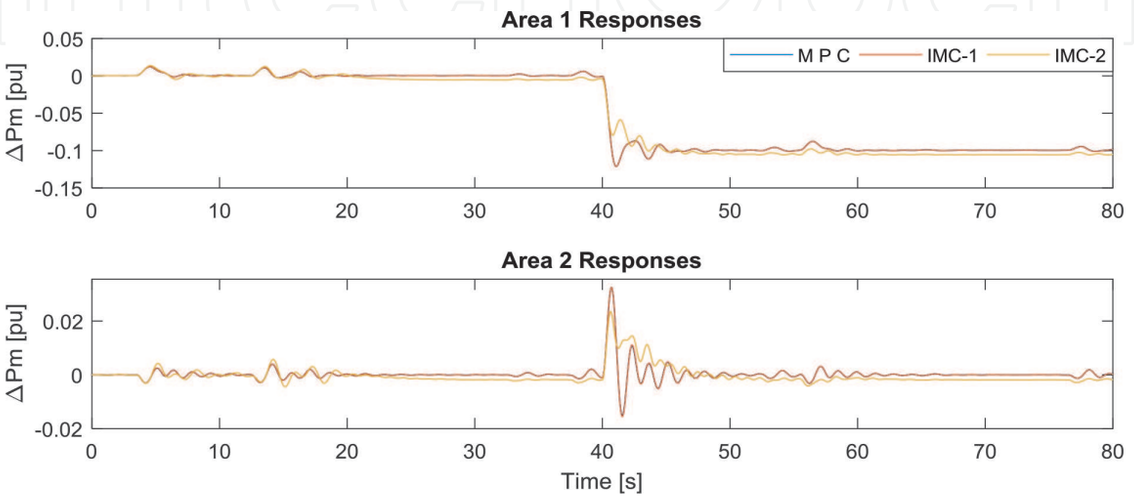


Figure 20.
Case 3: ΔP_m responses.

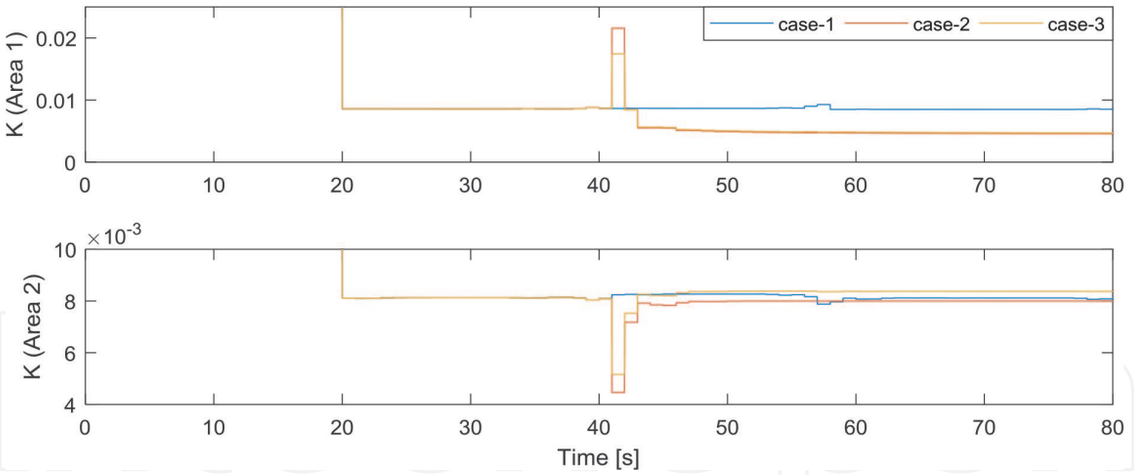


Figure 21.
Gain K *of IMC type 1.*

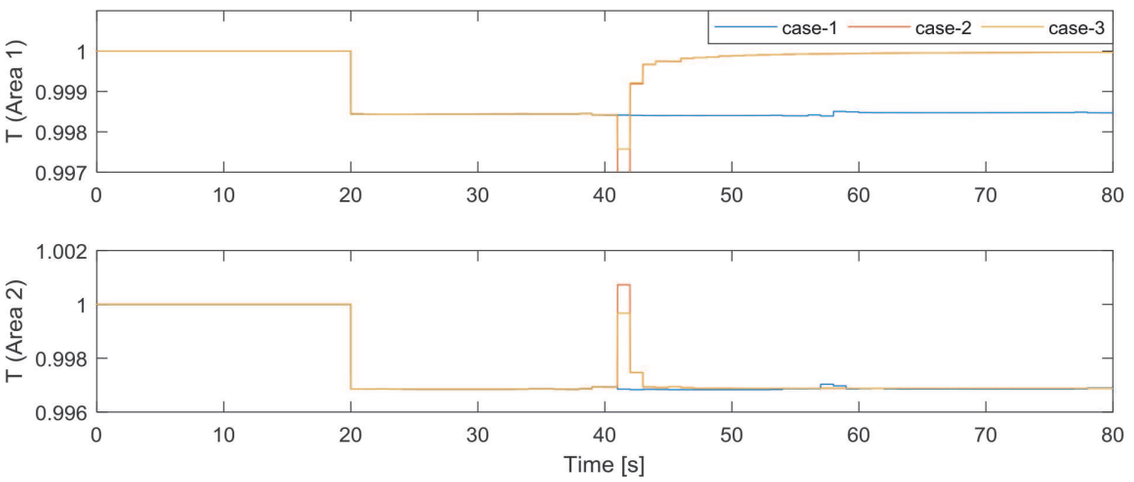


Figure 22.
Time constant T *of IMC type 1.*

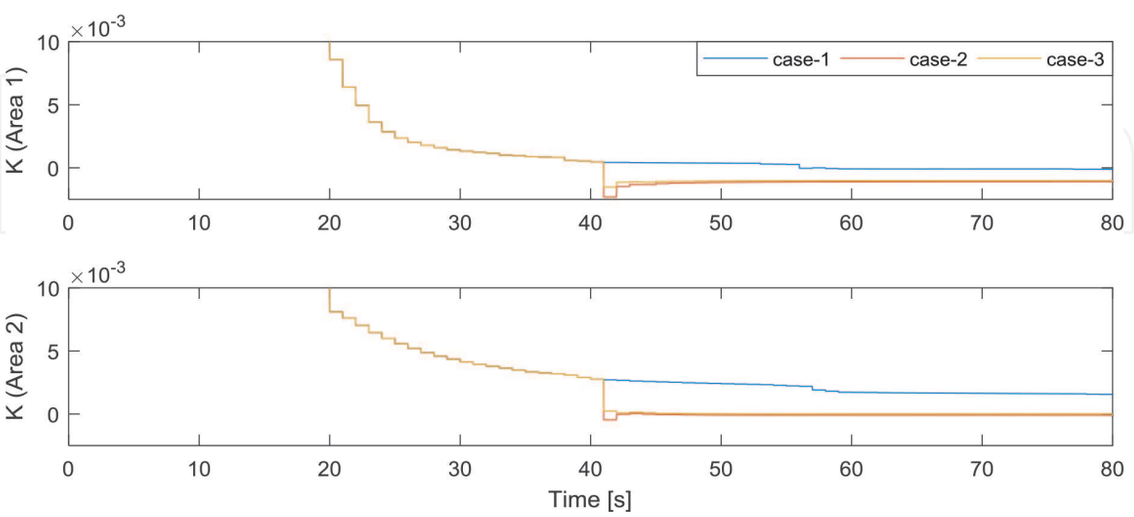


Figure 23.
Gain K *of IMC type 2.*

and handle the power system disturbances. In the same way, the controllers keep the system conditions successfully at the set points.

The simulations are carried out on PC with Intel Core i7 1.8 GHz CPU and 4 GB RAM using MATLAB 2016a under Windows 10. CPU times for the computation of

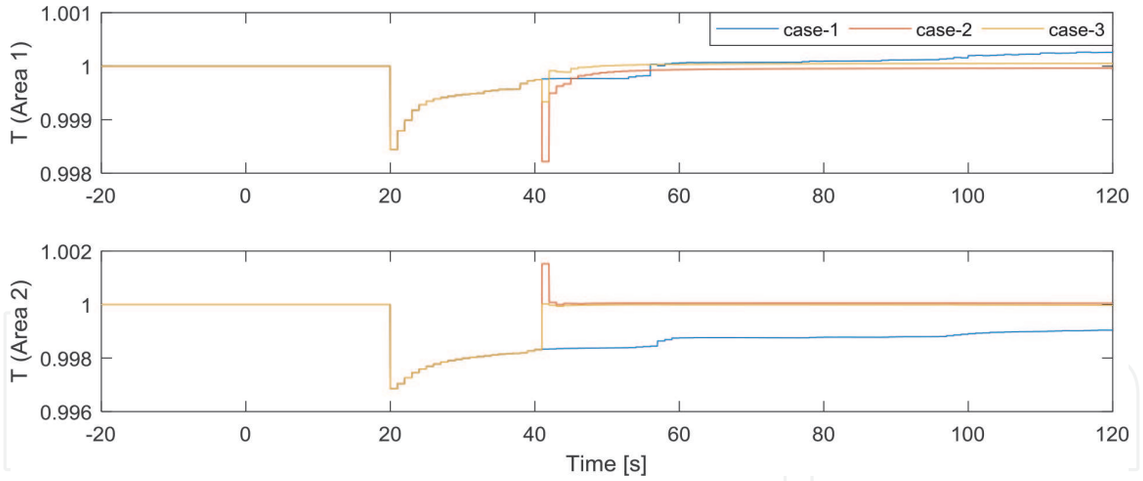


Figure 24.
Time constant T *of IMC type 2.*

Properties	Controller type	Case 1		Case 2		Case 3	
		Area 1	Area 2	Area 1	Area 2	Area 1	Area 2
Overshoot	MPC	0.1143	0.1339	0.1643	0.1008	0.0194	0.0143
	IMC-1	0.1139	0.1348	0.1643	0.1009	0.0193	0.0144
	IMC-2	0.0891	0.0362	0.1295	0.0393	0.0210	0.0203
Standard deviation	MPC	0.0186	0.0119	0.0094	0.0062	0.0033	0.0022
	IMC-1	0.0186	0.0120	0.0094	0.0063	0.0033	0.0022
	IMC-2	0.0131	0.0050	0.0073	0.003	0.0031	0.0019

Table 3.
Frequency responses.

Properties	Controller type	Case 1		Case 2		Case 3	
		Area 1	Area 2	Area 1	Area 2	Area 1	Area 2
Overshoot	MPC	0.2472	0.0302	0.0121	0.0325	0.0123	0.0039
	IMC-1	0.2472	0.0309	0.0122	0.0325	0.0124	0.0040
	IMC-2	0.2027	0.0058	0.0136	0.0236	0.0136	0.0058
Standard deviation	MPC	0.0945	0.0034	0.0466	0.0018	0.0018	0.0006
	IMC-1	0.0946	0.0034	0.0466	0.0018	0.0018	0.0006
	IMC-2	0.0913	0.0041	0.0485	0.0020	0.0028	0.0011

Table 4.
Prime mover responses.

Case	MPC	IMC-1	IMC-2
1	13.3645	16.6271	22.0835
2	13.6594	17.0485	23.0585
3	13.6208	16.7182	22.2260

Table 5.
Simulation time (s).

controllers are listed in **Table 5**. It is observed that the adaptive LFC controllers are slower than the conventional method.

In today's power system condition, where smart grid and energy management system are applied, the power system dynamics is varying. Therefore an adaptive model would be an advantage and is required for the better performance of LFC system.

It is observed that time consuming is increased together with the improvement of the controller performances. Therefore the IMC type 2 controller needs more time to compute and update both internal model and controller gain while giving a better performance. On the other hand this time consuming is the order of milli-second and so it is acceptable for an LFC system which in general operated in the order of second. Therefore the proposed controller has bit complexities in hardware for computing the model and updating the controller since its consuming time is about 40% higher than the existing MPC controller.

5. Conclusions

This chapter presents adaptive LFC methods based on IMC controller structure, where the internal model is adaptively updated online in IMC type 1, while both internal model and MPC controller gain are restructured in IMC type 2 by using the least square method. The performance of the controller is fair in handling load disturbances in spite of relatively slow control cycle with ramp rate constraints of actual systems.

Simulation results show that the gain and time constant of the internal model have been adaptively changed. This change has guaranteed the better performance of the proposed controller. Based on the system responses, the adaptive IMC controller type 1 has responses similar to the existing MPC controller, while the adaptive IMC controller type 2 has shown its superiority compared to MPC controller and IMC type 1 controller. In contrary, consuming time becomes larger by the enhancement of the controller performance.

Author details

Adelhard Beni Rehiara[1*], Naoto Yorino[2], Yutaka Sasaki[2] and Yoshifumi Zoka[2]

1 Electrical Engineering Department, University of Papua, Indonesia

2 System Cybernetics Department, University of Hiroshima, Japan

*Address all correspondence to: a.rehiara@unipa.ac.id

IntechOpen

© 2020 The Author(s). Licensee IntechOpen. Distributed under the terms of the Creative Commons Attribution - NonCommercial 4.0 License (https://creativecommons.org/licenses/by-nc/4.0/), which permits use, distribution and reproduction for non-commercial purposes, provided the original is properly cited. BY–NC

References

[1] Rehiara AB, Chongkai H, Sasaki Y, Yorino N, Zoka Y. An adaptive internal model for load frequency control using extreme learning machine. TELKOMNIKA. 2018;**16**:1-6

[2] He C, Rehiara AB, Sasaki Y, Yorino N, Zoka Y. The Application of Laguerre Functions Based Model Predictive Control on Load Frequency Control. In: the International Conference on Electrical Engineering (ICEE2018). Seoul, Republic of Korea; 2018. pp. 1190-1195

[3] Rehiara AB, Sasaki Y, Yorino N, Zoka Y. A performance evaluation of load frequency controller using discrete model predictive controller. In: 2016 International Seminar on Intelligent Technology and Its Applications. Lombok, Indonesia; 2016. pp. 659-664

[4] Rehiara AB, Chongkai H, Sasaki Y, Yorino N, Zoka Y. An adaptive IMC-MPC controller for improving LFC performance. In: 2017 IEEE Innovative Smart Grid Technologies—Asia. Auckland, New Zealand; 2018. pp. 1-6

[5] Abdillah M, Setiadi H, Rehiara AB, Mahmoud K, Farid IW, Soeprijanto A. Optimal selection of LQR parameter using AIS for LFC in a multi-area power system. Journal of Mechatronics, Electrical Power, and Vehicular Technology. 2016;7(2):93

[6] Kundur P. Power System Stability and Control. USA: McGraw Hill; 1993

[7] El-Hawary ME. Electrical Power Systems. New Jersey: Prentice-Hall; 1983

[8] Mohamed TH, Morel J, Bevrani H, Hiyama T. Model predictive based load frequency control-design concerning wind turbines. International Journal of Electrical Power & Energy Systems. 2012;**43**(1):859-867

[9] Mohamed TH, Hassan AA, Bevrani H, Hiyama T. Model predictive based load frequency control design. In: 16th International Conference on Electrical Engineering. 2010

[10] Wong C, Mears L, Ziegert J. Dead time compensation for a novel positioning system via predictive controls and virtual intermittent setpoints. In: 2009 International Manufacturing Science and Engineering Conference. Indiana, USA; 2009. pp. 1-8

[11] Wang L. Model Predictive Control System Design and Implementation Using MATLAB. London: Springer-Verlag; 2009

[12] Rehiara AB, Yorino N, Sasaki Y, Zoka Y. A novel adaptive LFC based on MPC method. IEEJ Transactions on Electrical and Electronic Engineering. 2019;**14**(8):1145-1152

[13] Shigemasa T, Yukitomo M, Kuwata R. A model-driven PID control system and its case studies. Proceedings of International Conference on Control Applications. 2002;**1**:571-576

[14] Jin Q, Feng C, Liu M. Fuzzy IMC for unstable systems with time delay. In: 2008 IEEE Pacific-Asia Workshop on Computational Intelligence and Industrial Application. Washington DC, USA; 2008. pp. 772-778

[15] Skala V. Least square method robustness of computations: What is not usually considered and taught. In: Proceedings of the 2017 Federated Conference on Computer Science and Information Systems, FedCSIS. Prague, Czech Republic; 2017. pp. 537-541

[16] More AN, Kohli PS, Kulkarni KH. Simple linear regression with least square estimation: An overview. International Journal of Computer

Science and Information Technologies. 2016;7(6):2394-2396

[17] Sivanagaraju S, Sreenivasan G. Power System Operation and Control. 1st ed. Delhi: Pearson Education; 2010

[18] He C, Rehiara AB, Sasaki Y, Yorino N, Zoka Y. Model predictive load frequency control using unscented Kalman filter. In: IEEJ Technical Meeting on Power Engineering. Jeju Island, Republic of Korea; 2018

IntechOpen